Presented at the 24th European PV Solar Energy Conference and Exhibition, 21-25 September 2009, Hamburg, Germany

LASER ABLATION OF ANTIREFLECTION COATINGS FOR PLATED CONTACTS YIELDING SOLAR CELL EFFICIENCIES ABOVE 20 %

Annerose Knorz, Monica Aleman, Andreas Grohe, Ralf Preu, Stefan W. Glunz
Fraunhofer Institute for Solar Energy Systems
Heidenhofstr. 2, 79110 Freiburg, Germany
Phone number: +49 – (0)761 4588 5499
Fax: +49- (0)0761 4588 9250
Email: annerose.knorz@ise.fraunhofer.de

ABSTRACT: To reduce shadowing losses and therefore gain higher short current densities J_{SC} as well as to overcome contact resistance limitations a front side metallization based on laser ablation of the antireflection coating and plated contacts is proposed. In this paper we will present solar cells with efficiencies of up to 20.7 % featuring an industrially feasible shallow diffused 110 Ohm/sq. emitter and a plasma enhanced chemical vapour deposition (PECVD)-SiN antireflection coating. The main focus in this paper lies on the laser ablation process. The characteristics of ns- and ps-laser ablation regarding the influence on the emitter profile and the ablation pattern on a textured surface will be discussed.
Keywords: Laser processing, metallization, solar cell

1 INTRODUCTION

For several reasons an alternative to the screen-printed front side metallization in the industrial production of solar cells is needed. The front side metallization process scheme as suggested by Dubé et al. [1] consisting of selective laser ablation of the antireflection (ARC) coating and plated contacts can reduce shadowing losses due to an improved aspect ratio and smaller finger widths. This leads to an increase of the short current density j_{SC} of every solar cell independent of the bulk quality. Due to the reduced contact resistance of the applied nickel silicide contact a high phosphorus concentration at the surface is not required and therefore an emitter with a high V_{OC}-potential can be used. Besides these advantages of the laser-based metallization scheme which lead to higher efficiencies, it does not need a high temperature step for the contact formation and is also contactless. This reduces the risk of wafer breakage which becomes increasingly important as wafer thickness is reduced. The absence of a high temperature step offers

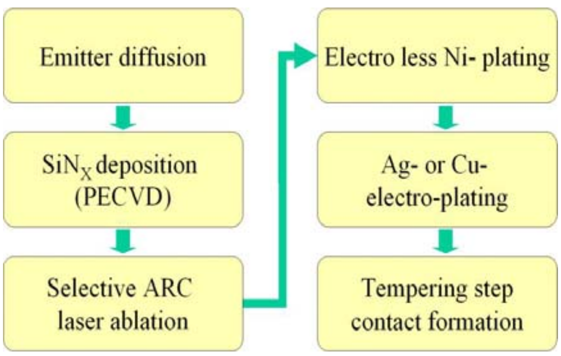

Figure 1: Process scheme for the low temperature front side metallization scheme featuring selective laser ablation and plated contacts.

the possibility to use materials which are not high temperature stable like amorphous silicon as passivation layers. In this paper we present solar cells with efficiencies of up to 20.7 % featuring a shallow diffused emitter. The front contacts were plated following selective laser ablation of the antireflection coating. The process scheme for the front side metallization can be seen in Figure 1. As the main focus in this paper lies on the laser ablation procedure, the characteristics of ps- and ns-laser ablation at a wavelength of 355 nm regarding the ablation structure and the influence on the emitter profile are discussed.

2 EXPERIMENTAL

2.1 SIMS-profiles

During the ablation of the antireflection coating the silicon beneath is heated and molten. The melt depth strongly depends on the pulse energy, the pulse width and wavelength of the laser. Since diffusion in a liquid is much faster than in a solid [2,3], the melting of silicon during the ablation process can lead to significant changes in the emitter profile of the contact area. This change will be especially strong with a shallow diffused emitter due to the high concentration gradient. To investigate the alteration in the emitter profile, shiny etched float zone wafers were diffused with a shallow 50 Ω/sq. emitter, coated with a 70 nm thick antireflection SiN-layer (n≈2.1) and ablated at different intensities with ns- and ps-pulses. Both lasers feature a wavelength of 355 nm and pulse widths of 30 ns and 12 ps respectively. The lasers, a Coherent Avia-355-x and a Lumera Super Rapid, are mounted on an InnoLas laser system which delivers the beam to the sample via a gantry system. The intensity was changed by keeping the pulse energy constant while varying the distancefrom the surface to the focal position. Afterwards secondary ion mass spectrometry (SIMS)-profiles of the ablated samples and a reference sample were measured. The phosphorus concentration of the ps- and ns-ablated samples compared to the emitter profile after diffusion is shown in Figure 2.

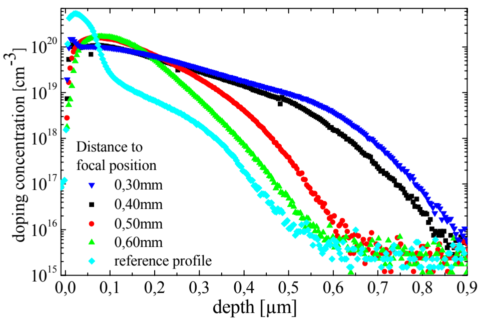

(a)

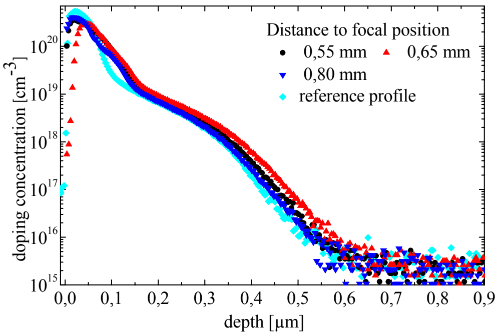

(b)

Figure 2: SIMS-profiles showing the phosphorus-concentration in dependence of the distance to the surface. Picture 2a shows the doping profiles of the reference sample and samples structured by ns-laser pulses, 2b shows the profiles of ps-laser structured samples.

The doping profiles of the ns-ablated samples show a deeper diffused emitter profile with increasing intensity. Higher intensities result in an increased melt depth and therefore a redistribution of the phosphorus content from the surface to deeper layers. For the ps-ablated samples the emitter profile does not differ from the original profile, keeping the distinguished kink and tail form. Since the laser material interaction takes place in such a short time, almost no heat diffuses into the material and the energy is used completely for the ablation. Therefore the melting of silicon is restricted to the surface and the emitter profile is preserved.

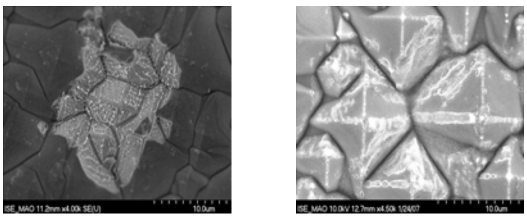

(a) (b)

Figure 3: SEM-pictures of ps- (a) and ns- (b) ablated antireflection coating on textured surfaces.

2.2 ns- and ps-ablation structure

As presented in [4] the ablation structure of an antireflection coating on a textured surface is dominated by interference and light trapping effects. For ns-laser ablation at low intensities the resulting amplifications in the electro-magnetic field lead to an incomplete opening of the antireflection coating (see Figure 3). Ps-laser ablation causes a rapid heating in the silicon due to the short interaction time which expands and thereby lifts off the antireflection coating completely. The amplifications in the electro-magnetic field are still visible in the damaged surface.

3 SOLAR CELL RESULTS

3.1 Solar cell structure

The processed solar cell structure features seven 20x20 mm² cells on four inch 250 µm thick 1 Ω cm p-type float zone silicon wafers. The planar rear side is passivated by a layer of 105 nm thermally grown SiO_2, covered by a 2 µm thick evaporated aluminum layer. The rear contacts are established by the LFC technology [5]. The $POCl_3$ diffused shallow emitter has a sheet resistance of approx. 110 Ω/sq. and uses no additional drive-in process. The front side is textured by random pyramids and coated with a 70 nm silicon nitride ARC deposited by PECVD. The selective laser ablation of the antireflection coating was performed using the above described ns- and ps-lasers. The contact grid consists of 25 fingers with a finger width of 30 µm for the ps-laser ablation, 20 µm for the ns-laser ablation and a 200 µm bus bar for both. After the laser ablation a Ni- seed layer was deposited and the contact was formed during a tempering step [6]. To thicken the contacts electro Ag-plating was used. Figure 4 shows microscopy pictures of the ps- and ns-pulse structured surface for the finger contacts. The ps-laser ablation is about 10 µm wider than the ns-laser ablation and the area fraction of the ablated antireflection coating is a lot higher (indicated by more bright areas). In Figure 5 a SEM – picture of a plated contact is shown.

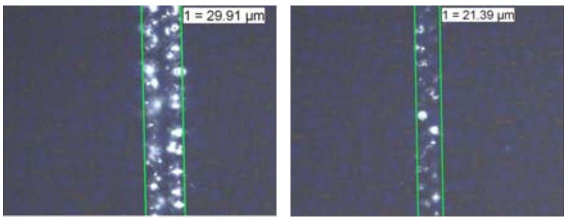

(a) (b)

Figure 4: Microscopy pictures of the laser ablated antireflection coating (a) shows the ps- and (b) the ns-structured surface.

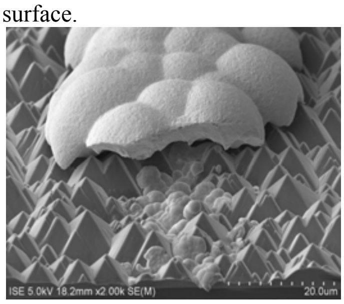

Figure 5: SEM-pictures of a laser ablated and plated finger.

As a reference to this process a sophisticated laboratory type front side metallization was chosen. The definition of the 30 μm wide contact area of the reference cell was done by photolithography. The antireflection coating was etched wet chemically followed by evaporating a TiPdAg-seed layer and a lift-off process. The thickening of the contacts again was performed in an Ag-electro plating process identical to the laser ablated samples.

Table 1: Results of the best PERC solar cells with a laser ablated antireflection coating and plated Ni-contact as well as a reference cell. FW represents the width of the ablated openings for the fingers.

Laser type	FW [μm]	V_{oc} [mV]	J_{sc} [mA/cm^2]	FF [%]	η [%]
ns	20	651	39.4	80.7	20.7
ps	30	634	38.7	80.0	19.7
ref	30	647	39.2	81.5	20.7

3.2 Solar cell characterization

The solar cells were characterized by light and dark IV-measurements. The results of the best ns- and ps-cell as well as a reference cell are shown in Tab. 1. The ns-laser ablated cell reaches the same level as the photolithography processed reference cell. Both cells have high fill factors and short current densities j_{SC} which result in a 20.7 % conversion efficiency. The best ps-ablated cell shows reduced open circuit voltage V_{OC} and a lower fill factor. The loss in V_{OC} is a result of a higher dark current density leading to higher recombination at the contacts as can be seen from the data in Tab.2 received from the dark IV-characteristics.

Table 2: Dark current densities extracted from fitting the dark IV-characteristics and the calculated maximal V_{OC}

Laser type	n_1	J_{01} [A/cm^2]	$V_{oc, max}$ [mV]	V_{oc} [mV]
ns	1	3.58 10^{-13}	658	651
ps	1	6.51 10^{-13}	642	634

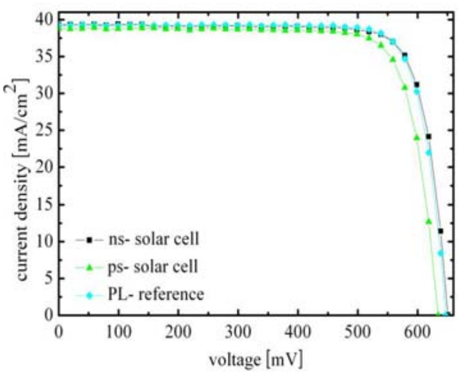

Figure 6: Light IV – characteristic of the best ps-, ns-ablated and reference cell.

The increased recombination is caused by the increased contact area compared to the ns-ablated cells as well as the fact that the emitter profile is not driven further into the material during laser ablation as well as a heavier damaged surface layer. The increased contact area is caused by the higher finger width as well as the complete removal of the antireflection during ps-laser ablation. As the emitter profile is not changed by the ps-ablation the laser induced damage is located closer to the space charge region compared to the ns-laser ablation. The losses can be seen by analysing the light IV-curves of the solar cells in Figure 6.

Since ps-laser ablation removes the antireflection coating in the irradiated area completely only a very small finger width is needed to avoid series resistance losses. This could be realized by only one line of laser pulses leading to competitive process cycle times. Since the surface is rough due to the rapid heating and cooling of the silicon and the antireflection coating is removed completely, the adhesion of the plated seed layer is better. If the ablated finger width is optimized for the ps-ablation and the fraction of the contact area is reduced, higher V_{OC} and efficiencies can be realized. As can be seen in Figure 7, the internal quantum efficiency is not significantly worse compared to the IQE of the reference cell.

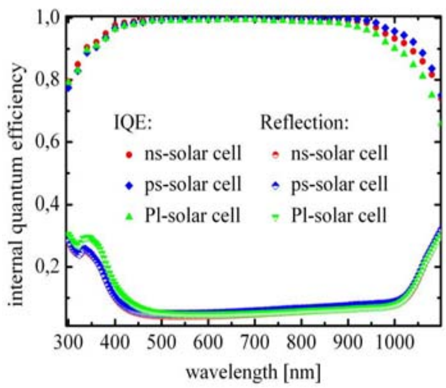

(a)

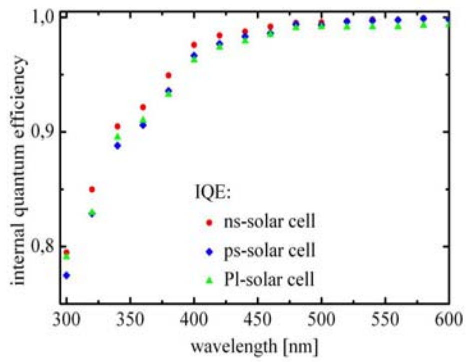

(b)

Figure 7: Internal quantum efficiencies of the best ps-, ns-ablated and reference solar cells.

4 CONCLUSION

Selective laser ablation of the antireflection layer can be a key process for an industrial feasible front side metallization scheme with plated contacts. In this paper the difference between ps- and ns-laser ablation regarding the ablation structure and influence on the emitter profile were discussed. Additionally solar cell results were presented with efficiencies of up to 20.7 % for ns-laser ablated cells and 19.7 % for ps-laser ablated cells. With the ns-laser ablation process the level of a photo lithographically defined and wet chemically opened reference could be reached. The ps-laser ablation process has still potential for higher efficiencies if the ablated area is reduced further.

5 ACKNOWLEDGEMENTS

The authors would like to thank S. Seitz, T. Leimenstoll, N. Kohn, M. Schwarzkopf, P. Hartmann and E. Schäffer for process technology and measurements.

6 REFERENCES

[1] C.E. Dubé, R.C. Gonsiorawski, “Improved contact metallication for high efficiency EFG polycrystalline silicon solar cells”; Proceedings of the 21st IEEE Photovoltaic Specialists Conference (1990)

[2] A. Bentzen, “Phosphorus diffusion and gettering in silicon solar cells ”; PhD thesis, Oslo Norway (2006)

[3] H. Kodera, “Diffusion Coefficients of Impurities in Silicon Melt”, Jap. J. Appl. Phys. Vol 2, p. 212-219, (1963)

[4] A. Knorz et al., “Selective laser ablation of SiN_X Layers on textured surfaces for low temperature front side metallization”; Prog. Photovolt: Res. Appl. 2009; 17::127-136

[5] R. Preu, E. Schneidelöchner, A. Grohe, S.W. Glunz, G. Willeke; “Laser-fired contacts - transfer to a simple high efficiency process scheme to industrial production”; Proceedings of the 29st IEEE Photovoltaic Specialists Conference, New Orleans, Louisiana, USA (2002)

[6] M. Aleman et al.; “Characterization of electroless nickel plating on silicon solar cells for the front side metallization”; Proceedings of the 22nd European Photovoltaic Solar Energy Conference, (2007) p. 1590-2